Journal of General Virology (2007), **88**, 3067–3077 **DOI** 10.1099/vir.0.82856-0

Severe acute respiratory syndrome coronavirus Orf3a protein interacts with caveolin

Kartika Padhan,[1] Charu Tanwar,[1] Amjad Hussain,[1] Pui Yan Hui,[2] Man Yan Lee,[2] Chung Yan Cheung,[2] Joseph Sriyal Malik Peiris[2] and Shahid Jameel[1]

Correspondence
Shahid Jameel
shahid@icgeb.res.in

[1]Virology Group, International Centre for Genetic Engineering and Biotechnology (ICGEB), Aruna Asaf Ali Marg, New Delhi 110 067, India

[2]Department of Microbiology, Queen Mary Hospital, University of Hong Kong, Hong Kong SAR

The *orf3a* (also called X1 or U274) gene is the largest unique open reading frame in the severe acute respiratory syndrome coronavirus genome and has been proposed to encode a protein with three transmembrane domains and a large cytoplasmic domain. Recent work has suggested that the 3a protein may play a structural role in the viral life cycle, although the mechanisms for this remain uncharacterized. Here, the expression of the 3a protein in various *in vitro* systems is shown, it has been localized to the Golgi region and its membrane topology in transfected cells has been confirmed. Three potential caveolin-1-binding sites were reported to be present in the 3a protein. By using various biochemical, biophysical and genetic techniques, interaction of the 3a protein with caveolin-1 is demonstrated. Any one of the potential sites in the 3a protein was sufficient for this interaction. These results are discussed with respect to the possible roles of the 3a protein in the viral life cycle.

Received 17 January 2007
Accepted 29 June 2007

INTRODUCTION

The aetiological agent for severe acute respiratory syndrome (SARS) was found to be a novel coronavirus (Ksiazek *et al.*, 2003; Marra *et al.*, 2003; Rota *et al.*, 2003). Like other members of this viral family, the SARS coronavirus (SARS-CoV) has an approximately 30 kb, positive-sense RNA genome that contains 14 potential open reading frames (ORFs) (Marra *et al.*, 2003; Rota *et al.*, 2003). As well as the genes responsible for virus structure and RNA replication, coronaviruses also carry several putative accessory genes whose functions are poorly characterized. These genes are generally dispensable for growth in cell culture, but appear to play roles in viral pathogenesis *in vivo* (de Haan *et al.*, 1999; Ortego *et al.*, 2003; Paul *et al.*, 1997; Wesley *et al.*, 1991).

In addition to the genes found in other coronaviruses, the SARS-CoV genome also contains nine unique putative ORFs (Marra *et al.*, 2003; Rota *et al.*, 2003). The region between the S and E genes in the SARS-CoV genome contains a locus found frequently in other coronaviruses that has been proposed to be important for virulence and pathogenesis (Wesley *et al.*, 1991; Vaughn *et al.*, 1995; Zeng *et al.*, 2004). In SARS-CoV, *orf3a*, also called *X1* (Rota *et al.*, 2003) or *U274* (Tan *et al.*, 2004b), is the largest of these ORFs and encodes a protein of 274 aa. It was predicted to contain an N-terminal signal peptide, followed by three transmembrane domains and a C-terminal cytoplasmic domain of approximately 150 aa (Zeng *et al.*, 2004). The 3a protein was localized to the plasma membrane and perinuclear regions of infected or transfected cells (Tan *et al.*, 2004b).

The 3a protein is associated with virus particles produced following infection of Vero E6 or CaCo2 cells (Ito *et al.*, 2005; Shen *et al.*, 2005) and assembles into virus-like particles when co-expressed with the M and E proteins in insect cells (Shen *et al.*, 2005). It is *O*-glycosylated (Oostra *et al.*, 2006), interacts with the M, E and S structural proteins (Tan *et al.*, 2004b) and forms inter-chain disulfide linkages with the S protein (Zeng *et al.*, 2004). The protein is released in membranous structures from transiently expressing, as well as SARS-CoV-infected, cells (Huang *et al.*, 2006) and the deletion of its gene reduces virus growth (Yount *et al.*, 2005). Convalescent sera from SARS patients contain antibodies to the 3a protein (Tan *et al.*, 2004a). In addition to a proposed structural role, the 3a protein may also have regulatory functions. The ectopic expression of 3a induces apoptosis in Vero E6 cells (Law *et al.*, 2005) and upregulates the expression of fibrinogen in A549 lung epithelial cells (Tan *et al.*, 2005). Recently, the 3a protein has been shown to possess ion-channel activity selective for monovalent cations and was proposed to belong to the viroporin class of proteins (Lu *et al.*, 2006).

The 3a protein may modulate the trafficking properties of the SARS-CoV spike (S) protein (Tan *et al.*, 2005). As well as the presence of tyrosine-sorting (YXXΦ) and diacidic motifs in its cytoplasmic region (Tan *et al.*, 2004b), the 3a

protein was also shown to contain putative binding sites for caveolin-1 (Cai *et al.*, 2003). The caveolins (1, 2 and 3) are 21–24 kDa proteins that form the major structural component of caveolae, which are membrane microdomains implicated in the uptake of small molecules through glycosylphosphatidylinositol (GPI)-anchored receptors (Rothberg *et al.*, 1992; Anderson, 1998). Caveolin-1 appears to play a direct role in caveolar biogenesis through its ability to form oligomers (Sargiacomo *et al.*, 1995; Schlegel & Lisanti, 2000) and its interaction with cholesterol (Murata *et al.*, 1995). Caveolae have also been proposed as sites for signal transduction (Razani *et al.*, 2000), virus entry into cells (Pelkmans *et al.*, 2001) and virus assembly (Brown *et al.*, 2002). The caveolar localization of various signalling molecules provides a compartmental basis for their subsequent regulated activation and also explains the cross-talk between different signalling pathways (Lisanti *et al.*, 1994). Many signalling molecules bind to and are regulated by caveolin-1 (Li *et al.*, 1996; Okamoto *et al.*, 1998; Smart *et al.*, 1999). The signalling pathways include the extracellularly regulated kinase (ERK) and inducible nitric oxide synthase (iNOS) pathways, two critical pathways involved in cell survival, proliferation and response to viral infection (Garcia-Cardena *et al.*, 1997; Engelman *et al.*, 1998, 1999; Felley-Bosco *et al.*, 2002). Caveolin also regulates the cell cycle through transcriptional repression of cyclin D1 (Hulit *et al.*, 2000) and a p53-dependent mechanism (Galbiati *et al.*, 2001).

In view of the presence of caveolin-1-binding motifs in the SARS-CoV 3A protein (Cai *et al.*, 2003) and the importance of caveolae in cell signalling, the cell cycle and virus uptake, we explored the interaction between caveolin-1 and the 3a protein. We show here the subcellular localization of the 3a proteins and their interaction with caveolin-1 by using various biochemical, genetic and biophysical methods.

METHODS

Materials. All common reagents were from Sigma unless stated otherwise. COS-1 cells were obtained from the ATCC (Manassas, VA, USA), whilst Madin–Darby canine kidney (MDCK) and HT29 cells were obtained from the National Animal Cell Repository (National Centre for Cell Sciences, Pune, India). All cell lines were cultured at 37 °C in 10 % CO_2 in complete Dulbecco's modified Eagle's medium (DMEM) containing 5 % fetal bovine serum (FBS). Anti-haemagglutinin (HA) tag and anti-enhanced GFP (EGFP) were from Santa Cruz Biotechnology, and anti-caveolin from Becton Dickinson Biosciences. Antibodies to 3a were prepared in rabbits immunized with a purified His_6-cyto3a protein (aa 125–274) expressed in *Escherichia coli*.

Plasmid constructs. The *orf3a* gene (nt 25 268–26 092) of the SARS-CoV genome (GenBank accession no. NC_004718) was provided by Dr Vincent Chow (National University of Singapore). Fragments corresponding to the full 3a or its cytoplasmic domain (aa 125–274) were cloned into the expression vector pSGI-HA to give pSGI-3a-HA and pSGI-cyto3a-HA. The pSGI-HA vector was derived from pSGI (Jameel *et al.*, 1996) by inserting annealed oligonucleotides carrying the HA epitope at the 3′ end of the multiple cloning sites, placing the HA tag at the C terminus of the 3a proteins. Mutants of 3a with deletions of individual caveolin-1-binding motifs were constructed by PCR-based mutagenesis of pSGI-3a-HA. These included single mutants Δ1 (aa 69–77; nt 205–231), Δ2 (aa 107–114; nt 319–341) and Δ3 (aa 141–149; nt 421–447) and the double mutants Δ1 + Δ2 and Δ2 + Δ3. The 3a cytoplasmic domain containing a deletion of the third potential caveolin-1-binding domain (Δ3cyto3a) was made by PCR amplification. All mutants were confirmed by DNA sequencing. For yeast two-hybrid assays and microscopy, the 3a fragments were cloned into plasmids pGBKT7 (as *Nco*I–*Bam*HI fragments) and pECFP-N1 (as *Eco*RI–*Bam*HI fragments), respectively. The 3a gene was cloned into plasmid pDsRed-N1 as an *Eco*RI–*Bgl*II fragment. The caveolin-1 gene (Schlegel & Lisanti, 2000) was cloned into plasmids pGADT7 (as an *Nco*I–*Bam*HI fragment) and pEYFP-N1 (as an *Eco*RI–*Bam*HI fragment) for two-hybrid assays and microscopy, respectively. The primer sequences, PCR conditions and cloning details are available upon request.

***In vitro* synthesis, transfection and detection.** For *in vitro* protein expression, a coupled transcription–translation system (TNT; Promega) was used according to the manufacturer's instructions, programmed with DNA from pSGI-HA-based plasmids as described previously (Jameel *et al.*, 1996). Transfections of animal cells, carried out with 5 μg plasmid DNA per 60 mm dish and Lipofectin (Invitrogen), and Western blotting were performed as described previously (Kar-Roy *et al.*, 2004).

Immunofluorescence, subcellular localization and fluorescence resonance energy transfer (FRET) assays. Cells grown on coverslips to 40–50 % confluence were transfected in antibiotic- and serum-free DMEM. Six hours post-transfection, the medium was removed and replaced with complete DMEM containing 5 % FBS. Around 48 h post-transfection, the cells were washed with PBS, fixed with 2 % paraformaldehyde for 15 min at room temperature and observed directly in the case of fluorescently tagged proteins, or stained with antibodies and imaged as described previously (Kar-Roy *et al.*, 2004). For subcellular localization, cells were co-transfected to express the required protein and a relevant fluorescent subcellular marker (Living Colours Subcellular Localization Vector set; Clontech). For FRET analysis, COS-1 cells were transfected as described above with 3a–enhanced cyan fluorescent protein (ECFP) (full-length, cyto or Δ3cyto) and caveolin-1–enhanced yellow fluorescent protein (EYFP) expression plasmids. Image acquisition and FRET assays were as described previously (Kar-Roy *et al.*, 2004). The percentage FRET efficiency was calculated by using the formula

$$\text{FRET efficiency (\%)} = 1 - \frac{(\text{ECFP intensity before photobleach})}{(\text{ECFP intensity after photobleach})} \times 100$$

Preparation and analysis of microsomes. The preparation of microsomal membranes from transfected cells, *in vitro* translation in the presence of canine pancreatic membranes (Promega) and protease protection of the translocated 3a protein were carried out essentially as described previously (Zafrullah *et al.*, 1999).

Triton solubility, alkaline carbonate extraction and caveolar fractions. The extraction of Triton X-100-soluble proteins and alkaline carbonate extraction were performed as described previously (Schlegel *et al.*, 1999). Transfected COS-1 cells were fractionated in the presence of Triton X-100 to isolate caveolar fractions as described previously (Cherukuri *et al.*, 2004; Sargiacomo *et al.*, 1993). Various fractions (20 μl each) were separated by SDS-PAGE and analysed by Western blotting.

Yeast two-hybrid assays. The 3a and caveolin-1 genes in the pGBKT7 and pGADT7 two-hybrid vectors, respectively, were used. Expression of the relevant fusion proteins was checked *in vitro* by using a TNT system (Promega). The yeast two-hybrid analysis was carried out essentially as described previously (Kar-Roy *et al.*, 2004; Tyagi *et al.*, 2004). The specificity of the interaction was tested as growth on plates containing 20 mM 3-amino-1,2,3-triazole (3AT). The filter-lift and liquid β-galactosidase assays were carried out as described previously (Kar-Roy *et al.*, 2004; Tyagi *et al.*, 2004).

RESULTS

Expression of the 3a proteins

The genes for full-length 3a protein, its cytoplasmic domain and various mutants with deletions in potential caveolin-1-binding motifs were cloned and verified by sequencing (Fig. 1a, b). Following cloning into the pSGI-HA vector, all constructs expressed proteins of the expected size in a coupled transcription–translation system (Fig. 1c). Expression was also tested in transfected COS-1 cells followed by either Western blotting or indirect immunofluorescence (IFA). Whilst high levels of 3a–HA expression were observed in transfected cell lysates (Fig. 2a), the Cyto3a–HA protein could not be detected by Western blotting (not shown). When transfected cells were observed by IFA, large numbers were repeatedly found to express 3a–HA, but very few cells expressed Cyto3a–HA (Fig. 2b). This was the case with multiple transfections, using different plasmid preparations and transfection reagents, suggesting that either the Cyto3a–HA plasmid was poorly transfected or the protein was degraded rapidly. The 3a–HA protein localized prominently to the perinuclear region; smaller amounts were also present on the plasma membrane. The Cyto3a–HA protein was, however, restricted to the perinuclear region, with none found at the plasma membrane.

Subcellular localization of the 3a protein

In COS-1 cells co-transfected to express 3a and an organelle-specific marker, the 3a protein was found to localize predominantly to the Golgi (Fig. 2c), but not to the endoplasmic reticulum or mitochondria (not shown). Three transmembrane domains are predicted in the 3a protein. To determine its topology on intracellular and

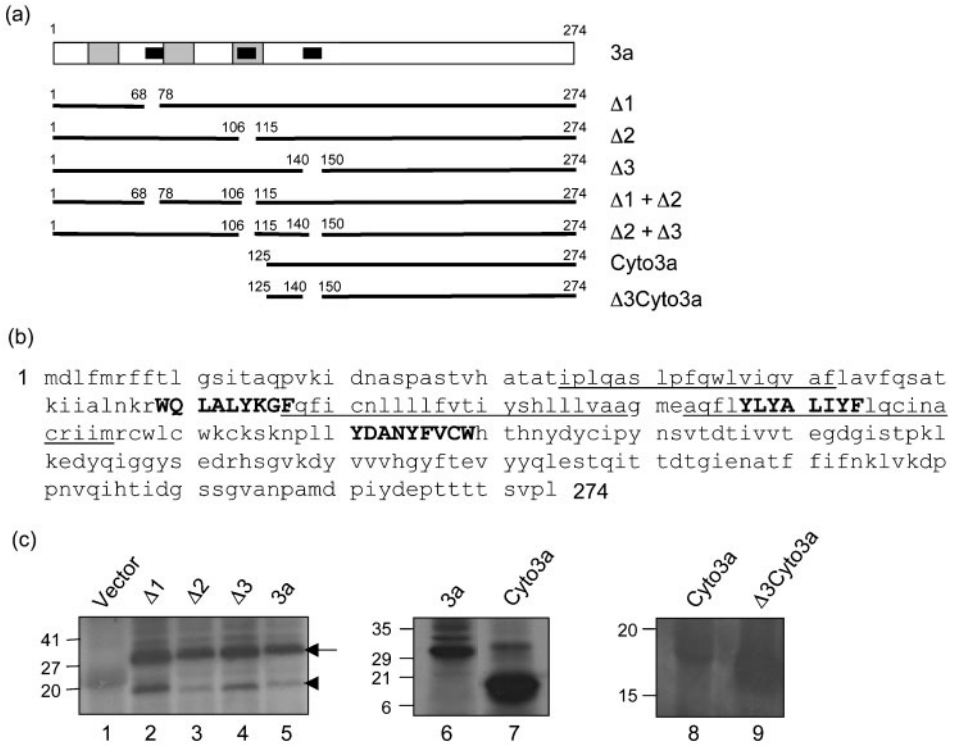

Fig. 1. Orf3a constructs used in this study. (a) The 3a protein (274 aa) is shown with its predicted transmembrane regions (grey boxes) and caveolin-binding motifs (black boxes). The various 3a deletion mutants used in this study are shown as lines, with breaks indicating the deleted regions. Numbers represent amino acid residues. (b) The amino acid sequence of the 3a protein is shown with the predicted transmembrane regions (underlined) and potential caveolin-binding motifs (bold, upper case). (c) *In vitro* coupled transcription–translation to confirm protein expression from the indicated pSGI-HA constructs. In the first panel (lanes 1–5), the arrow indicates the full-length protein; the arrowhead indicates the product of *in vitro* translation from an internal AUG codon. Size markers (kDa) are shown on the left of each panel.

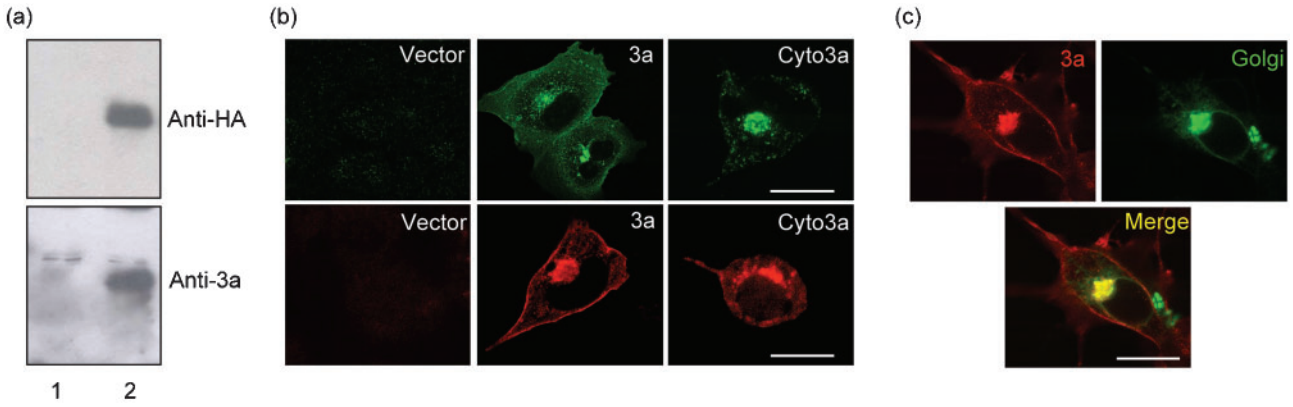

Fig. 2. Expression and subcellular localization of the 3a protein. (a) COS-1 cells were transfected with pSGI-HA vector (lane 1) or pSGI-3a-HA (lane 2) and the cell lysates were subjected to Western blotting with either anti-HA or anti-3a antibodies as described in Methods. (b) COS-1 cells were transfected with pSGI-HA (vector), pSGI-3a-HA or pSGI-Cyto3a-HA and the cells were stained for IFA with either anti-HA or anti-3a. (c) COS-1 cells were co-transfected with pSGI-3a-HA and pEYFP-Golgi. Cells were stained for 3a–HA expression with anti-HA and anti-rabbit–Alexa 594 antibodies, and imaged as described in Methods. The pseudocoloured images are shown individually and merged to show colocalization of 3a with the Golgi marker. Bars, 5 μm (b, c).

plasma membranes, we carried out trypsin-digestion experiments. The 3a–HA proteins were expressed *in vitro* in the presence of canine microsomal membranes and the vesicles were subjected to trypsin digestion to evaluate protection of the translocated proteins. Whilst the 3a–HA protein sedimented with the vesicles, it was not protected from trypsin digestion (Fig. 3a; lanes 4–6). In contrast, similarly synthesized and processed yeast α factor was protected from trypsin digestion in the absence, but not in the presence, of NP-40 (Fig. 3a; lanes 1–3). The status of translocated 3a–HA was also analysed by using microsomes prepared from transfected COS-1 cells. Again, no trypsin protection was observed (Fig. 3b). This suggests that the 3a protein either associates with the cytoplasmic face of membranes or inserts into membranes with a topology that places most of it outside the vesicles.

Colocalization of 3a and caveolin-1

There are three predicted caveolin-1-binding sites in 3a (Fig. 1b). To address whether 3a and caveolin-1 colocalize in cells, we carried out biochemical fractionations. Lysates from co-transfected cells were separated into Triton X-100-soluble and -insoluble fractions. The 3a–HA protein

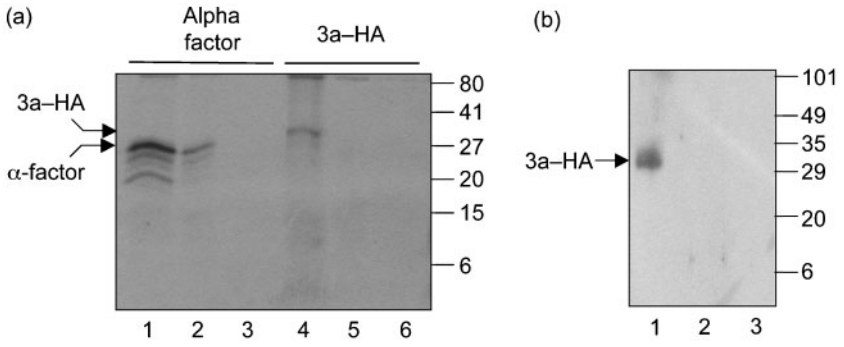

Fig. 3. Membrane topology of the 3a protein. (a) The yeast α-factor (lanes 1–3) or 3a–HA (lanes 4–6) proteins were synthesized *in vitro* in a T7 coupled transcription–translation system in the presence of canine pancreatic membranes. The microsomes were pelleted and subjected to trypsin digestion as described in Methods, and the proteins were detected by SDS-PAGE and fluorography. Lanes: 1 and 4, untreated; 2 and 5, with trypsin; 3 and 6, with trypsin and NP-40. Arrows indicate the undigested protein bands. (b) COS-1 cells were transfected with pSGI-3a-HA; the microsomes were prepared and treated with trypsin as described in Methods and the proteins were detected by Western blotting with anti-3a antibodies. Lanes: 1, untreated; 2, with trypsin; 3, with trypsin and NP-40. The 3a–HA band is indicated.

localized to the soluble fraction that also contained about 40–50 % of the endogenous caveolin-1 and a small fraction of caveolin-1–EGFP (Fig. 4a). The control EGFP–protein was found mainly in the soluble fraction. We then isolated caveola-enriched membrane fractions by sucrose-gradient ultracentrifugation of Triton X-100 lysates prepared from 3a–HA-expressing cells. Endogenous caveolin was present in two regions of the gradient: the top half, which represents cholesterol-rich membrane domains (rafts), and the bottom half, which represents non-raft membrane fractions (Fig. 4b). The 3a–HA protein was found in the same non-raft fractions as endogenous caveolin-1 (Fig. 4b). Proteins attached to the surface of membranes are solubilized easily by alkaline carbonate extraction, whereas integral membrane proteins remain insoluble. On alkaline carbonate extraction, caveolin as well as caveolin-1–EGFP were found mainly in the insoluble fraction, which also contained about 20 % of the 3a–HA protein (Fig. 4c). Thus, 3a and caveolin-1 were found to colocalize, based on Triton X-100 solubility, membrane flotation and alkaline carbonate extraction.

The colocalization of caveolin-1 and 3a was also assessed by confocal microscopy in three different cell lines (MDCK, HT29 and COS-1) that express variable amounts of caveolin-1. Extensive colocalization of caveolin-1 and 3a was observed as punctate, perinuclear staining, shown earlier to be in the Golgi region (Fig. 5a). This was also true for all the 3a mutants that lacked either one or two of the three potential caveolin-1-binding sites (Fig. 5b). The Cyto3a–HA protein also showed similar distribution but when aa 141–149, comprising the third potential caveolin-binding motif of 3a, were deleted, there was a dramatic change in its distribution (Fig. 5c). Instead of punctate staining, the Δ3Cyto3a–HA protein showed a diffuse cytoplasmic distribution (Fig. 5c) and did not colocalize with caveolin-1. These results suggest that the presence of just one of the three potential caveolin-1-binding motifs is sufficient for the characteristic subcellular distribution of 3a and its colocalization with caveolin-1.

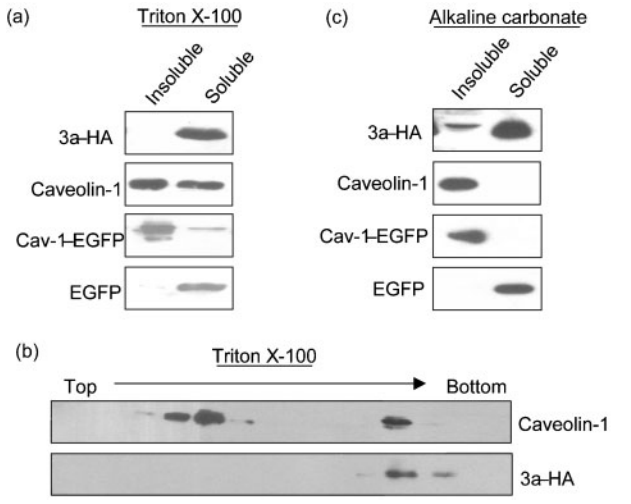

Fig. 4. Co-fractionation of 3a and caveolin-1. (a) COS-1 cells were co-transfected with pSGI-3a-HA and either pCav-1-EGFP or pEGFP-N1, treated with Triton X-100 and the insoluble and soluble fractions were Western blotted for 3a–HA, endogenous caveolin, Cav-1–EGFP or EGFP. (b) COS-1 cells transfected with pSGI-3a-HA were lysed with Triton X-100 and the lysates were subjected to ultracentrifugation to isolate caveola-enriched membrane fractions. Gradient fractions were analysed by Western blotting for caveolin-1 and 3a–HA proteins. (c) COS-1 cells were co-transfected as described in (a), subjected to alkaline carbonate extraction and the insoluble and soluble fractions were analysed for various proteins by Western blotting.

Yeast two-hybrid analysis of the caveolin-1–3a interaction

To assess any direct interaction between caveolin-1 and 3a, we used the yeast two-hybrid system as described in Methods. A representative set of plates is shown in Fig. 6(a). All transformants grew on non-selective yeast extract/peptone/glucose (YPD) plates. Single transformants and all co-transformants containing activation domain (AD)–caveolin-1 grew on SD/Leu$^-$ (L−) plates; similarly, those containing binding domain (BD)–3a grew on SD/Trp$^-$ (T−) plates and the co-transformants grew on SD/Leu$^-$Trp$^-$ (LT−) plates. Co-transformants that contain interacting protein pairs can transactivate the *HIS3* gene, resulting in growth on SD/Leu$^-$Trp$^-$His$^-$ (LTH−) plates. The growth of AD–caveolin/BD–3a co-transformants on the LTH− plate is indicative of an interaction between the two proteins. The transformants were also grown on LTH− plates in the presence of 20 mM 3AT to further confirm the specificity and strength of the interactions. All co-transformants that grew on LTH− plates also grew on the 3AT plates. Colonies were transferred to a nitrocellulose filter and a β-galactosidase filter assay was carried out. The presence of β-galactosidase activity only in the positive control and AD–caveolin/BD–3a co-transformants further confirmed the caveolin-1–3a interaction. The same analysis was repeated with AD–caveolin-1 and either BD–cyto3a or BD–Δ3cyto3a co-transformants (Fig. 6b). The results showed interaction of caveolin-1 with the cyto3a protein; this binding was lost when the caveolin-binding motif in cyto3A (aa 141–149) was removed (Fig. 6b). A semiquantitative liquid β-galactosidase assay also confirmed these results (not shown).

FRET for caveolin-1–3a interaction

To confirm these protein–protein interactions further *in vivo*, we carried out FRET assays. COS-1 cells were co-transfected with vectors expressing 3a–ECFP and caveolin-1–EYFP, as already shown in Fig. 5(a). To measure FRET, we followed an acceptor photobleach protocol, wherein the mean fluorescence intensities from the donor (ECFP) and acceptor (EYFP) fluorophores were recorded before and

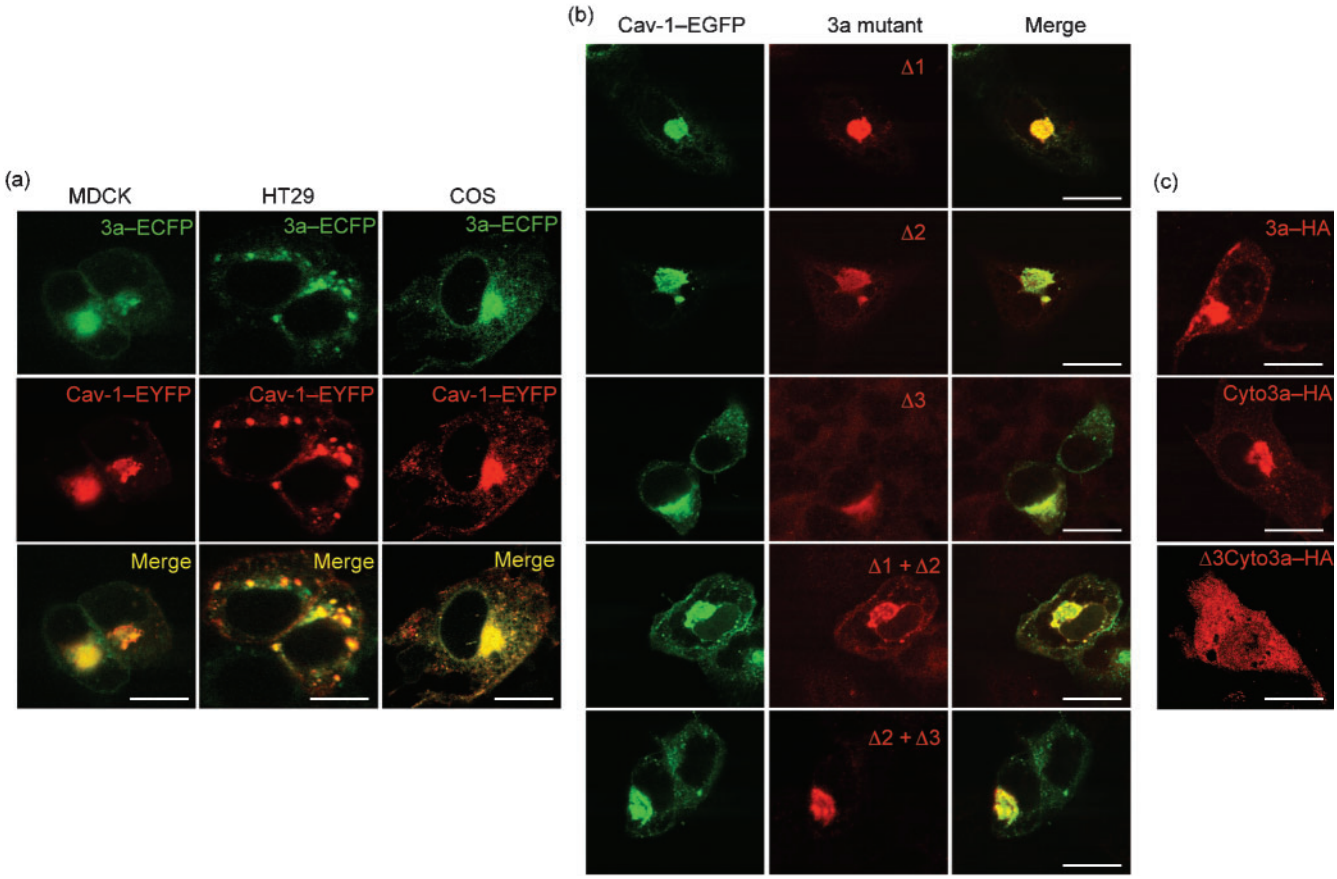

Fig. 5. Subcellular distribution of caveolin-1 and 3a proteins. (a) MDCK, HT29 and COS-1 cells were co-transfected with p3a-ECFP and pCav-1-EYFP and the cells were imaged for expression of the fluorescent fusion proteins. The ECFP and EYFP images are pseudocoloured green and red, respectively, and merged images are shown. (b) COS-1 cells were co-transfected with pCav-1-EGFP and one of the indicated 3a mutants in a pSGI-HA background. The transfected cells were stained with anti-HA antibodies and imaged for caveolin and 3a. (c) COS-1 cells were transfected with pSG-3A-HA, pSG-Cyto3A-HA or pSG-Δ3Cyto3A-HA expression constructs; the expressed proteins were stained with anti-HA antibodies. Bars, 5 μm.

after EYFP photobleaching (Siegel *et al.*, 2000; Xia & Liu, 2001). Two different areas within the same cell, one showing colocalization and another where no colocalization was observed, were subjected to FRET analysis. As expected, the 3a–ECFP and caveolin-1–EYFP proteins colocalized in transfected cells (Fig. 7a, upper panels). On simultaneous scanning of the two fluorophores, there was an increase in cyan (donor) fluorescence following bleaching of the yellow (acceptor) fluorophore (middle panels); this was also monitored in real time (lower panel). Similar measurements were also made in cells expressing caveolin-1–EYFP together with either Cyto3a–ECFP (Fig. 7b) or Δ3Cyto3a–ECFP (Fig. 7c). Multiple FRET measurements were carried out in more than one region of the same cell, with similar results. The mean fluorescence intensities were determined for each FRET measurement and the efficiency was calculated. Whilst there was efficient FRET between caveolin-1–EYFP and either 3a–ECFP or Cyto3a–ECFP, none was observed with Δ3Cyto3a–ECFP (table in Fig. 7). Thus, FRET analysis further confirmed direct binding of caveolin-1 to the 3a protein.

DISCUSSION

Several unique ORFs were predicted in the SARS-CoV genome (Marra *et al.*, 2003; Rota *et al.*, 2003). As this virus shows increased virulence compared with other human coronaviruses (Holmes, 2003; Navas-Martin & Weiss, 2003), it is reasonable to hypothesize a role for the unique SARS-CoV proteins in its pathogenesis, virulence or disease outcomes. The 3a protein is the product of the largest unique ORF in the SARS-CoV genome and is expressed during infection of human patients, as well as by cells in culture (Zeng *et al.*, 2004; Tan *et al.*, 2004a; Yu *et al.*, 2004).

By using 3a expression constructs, we show that a protein of the predicted size of approximately 34 kDa is expressed

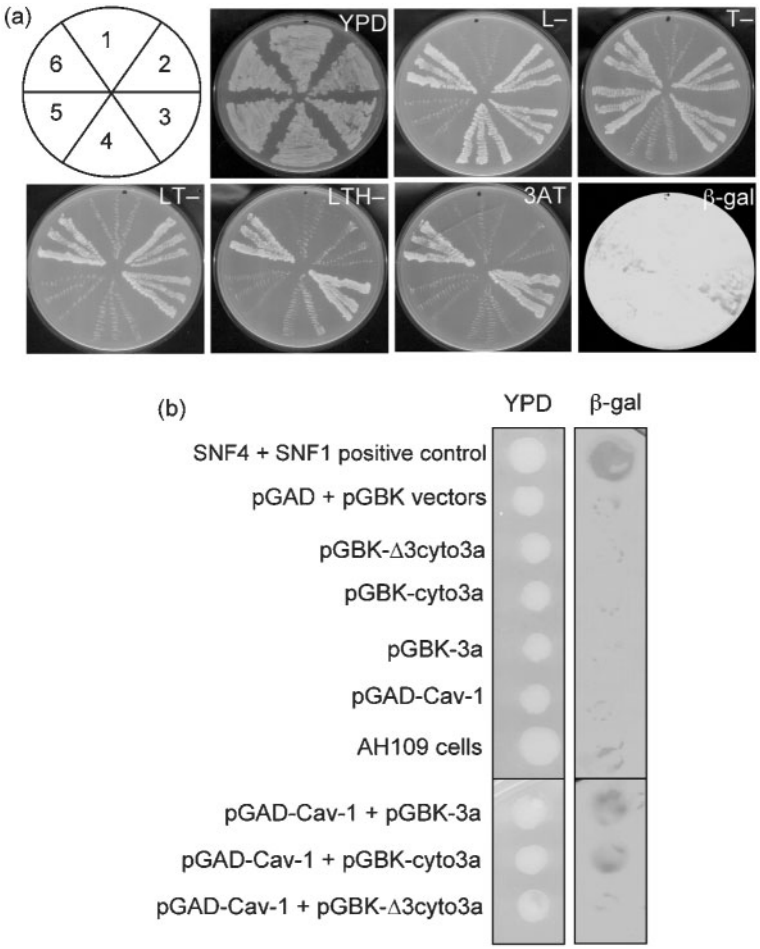

Fig. 6. Yeast two-hybrid analysis. (a) Representative plates showing the interaction of caveolin-1 with 3a. The first panel shows the template, whilst the remaining panels show transformants on the indicated medium plates. Growth is visible as light streaks on a dark background. The last panel shows results from the β-galactosidase (β-gal) filter assay, with the signal visible as dark streaks on a light background. The template shows: 1, AH109 cells; 2, pGAD and pGBK vectors; 3, SNF4 and SNF1 (positive control); 4, pGAD-Cav-1; 5, pGBK-3a; 6, pGAD-Cav-1 and pGBK-3a. (b) Growth of single or co-transformants on YPD plates followed by a filter-lift β-galactosidase assay. The dark spots show positive β-gal activity, indicative of interaction between proteins expressed by the co-transforming plasmids.

in transfected animal cells and localizes to the plasma membrane and Golgi region. This is in agreement with other reports (Tan *et al.*, 2004b; Yuan *et al.*, 2005). Whilst the cytoplasmic domain of 3a (aa 125–274) is not present on the plasma membrane, it still localizes to the Golgi. In another study, a cytoplasmic region of 3a that included aa 147–274 fused to EGFP did not show perinuclear localization, but was distributed throughout the cell in a pattern similar to EGFP (Yuan *et al.*, 2005). This suggested that, besides the transmembrane region, aa 125–147 of 3a were also critical for its characteristic subcellular distribution. This region contains a putative caveolin-1-binding site, YDANYFVCW (aa 141–149). In addition, two other caveolin-1-binding sites, WQLALYKGF (aa 69–77) and YLYALIYF (aa 107–114), were predicted within the 3a protein (Cai *et al.*, 2003). By using an N-terminally myc-tagged protein, Tan *et al.* (2004b) demonstrated the topology of the 3a protein to be such that its N terminus is extracellular and its C terminus is cytoplasmic. This would place the N terminus in the lumen of microsomal vesicles and leave the C terminus exposed to trypsin in our protection experiments. With 17 predicted trypsin-cleavage sites on the 3a protein, its complete digestion with this topology would result in fragments too small to be seen on the gels in Fig. 3. Alternatively, a reverse topology would produce a protected fragment of about 150 aa; this was clearly not observed. Thus, our results confirm earlier findings (Tan *et al.*, 2004b).

The 3a protein was predicted to be a transmembrane protein (Zeng *et al.*, 2004) and subsequent studies on its topology (Tan *et al.*, 2004b) and *O*-glycosylation (Oostra *et al.*, 2006) have supported this prediction. Whilst our results confirm the membrane topology of 3a, alkaline carbonate extraction reproducibly showed only about 20 % of the protein in the insoluble fraction. This, together with its complete solubility in Triton X-100, suggests that the 3a protein may have an unusual membrane insertion. The pestivirus E^{rns} (Fetzer *et al.*, 2005) and infectious bronchitis virus 3a (Pendelton & Machamer, 2005) are examples of proteins that are neither stripped easily with alkaline carbonate like peripheral membrane proteins, nor bound tightly like integral membrane proteins.

The Cyto3a protein (aa 125–274) is devoid of any predicted transmembrane domain, but still localized to the Golgi. It is possible that this accumulation is on the cytoplasmic face of the Golgi, possibly due to its interaction with another Golgi-associated protein. A

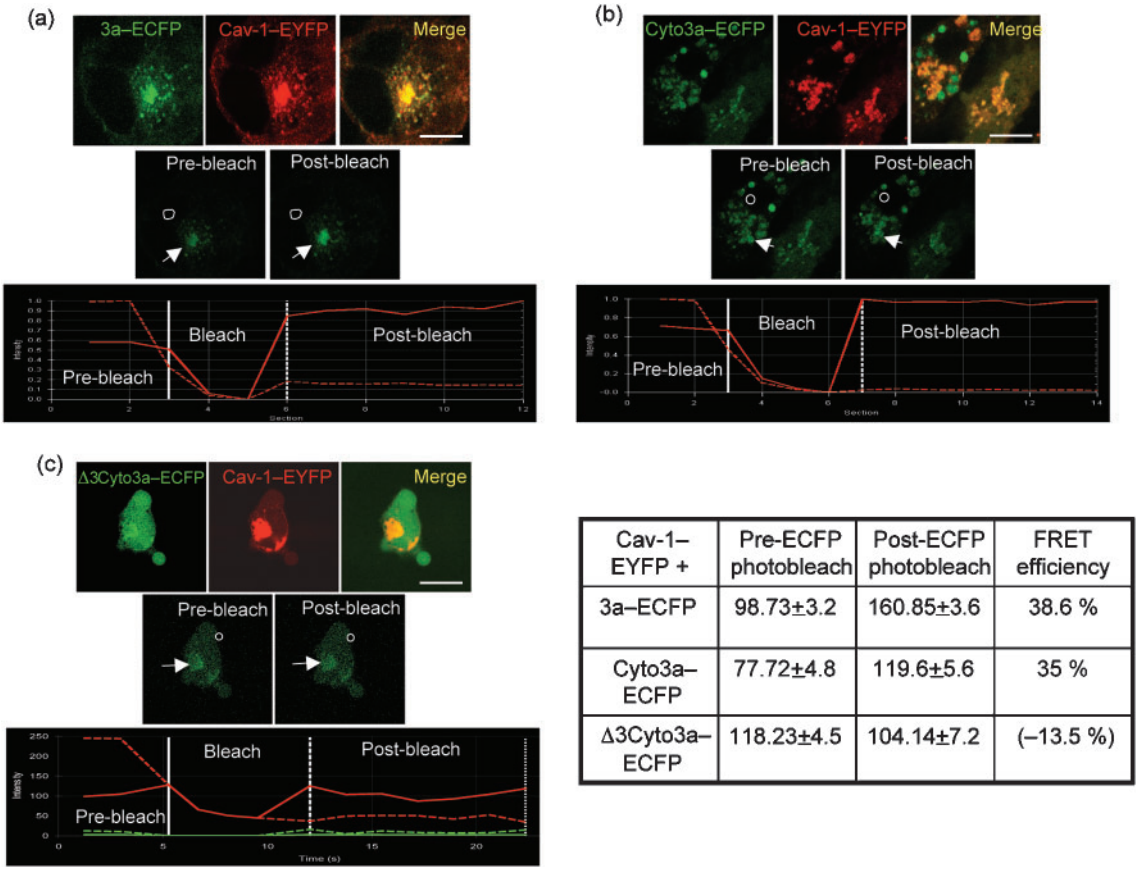

Cav-1–EYFP +	Pre-ECFP photobleach	Post-ECFP photobleach	FRET efficiency
3a–ECFP	98.73±3.2	160.85±3.6	38.6 %
Cyto3a–ECFP	77.72±4.8	119.6±5.6	35 %
Δ3Cyto3a–ECFP	118.23±4.5	104.14±7.2	(–13.5 %)

Fig. 7. FRET analysis of caveolin-1–3A interactions. (a) COS-1 cells were co-transfected to express the 3a–ECFP and Cav-1–EYFP fusion proteins as the donor–acceptor FRET pair. The pseudocoloured individual and merged images are presented (upper panels). Bar, 5 μm. Areas within the cell showing either colocalization (arrow) or no colocalization (circle) were bleached for EYFP, and ECFP images were acquired pre- and post-bleach (middle panels). A kinetic profile of the entire FRET experiment is also presented (lower panel). Fluorescence intensities of the ECFP (solid line) and EYFP (dashed line) fusion proteins during the three phases of the experiment are indicated. (b) As (a), except that the donor–acceptor FRET pair was Cyto3a–ECFP and Cav-1–EYFP. (c) As (a), except that the donor–acceptor FRET pair was Δ3Cyto3a–ECFP and Cav-1–EYFP. In the lower panel, green lines indicate intensities for the no-colocalization region. The table shows mean fluorescence intensities for ECFP before and after EYFP bleaching, and FRET efficiencies. A total of five independent FRET experiments were carried out in at least three different co-transfected cells each time. The images and intensities are representative of those experiments.

caveolin-binding site is predicted within the Cyto3a protein and caveolin is localized prominently to the Golgi. We carried out three different cell fractionation procedures to show that the 3a protein co-fractionated with both endogenous caveolin-1 and an ectopically expressed caveolin-1–EGFP fusion protein. Furthermore, by using fluorescent-protein-tagged caveolin and 3a, we demonstrated colocalization of these proteins in transfected cells. Deletion of any one or two of the three potential caveolin-1-binding motifs had no effect on this. Together with the distribution pattern of the Cyto3a and Δ3Cyto3a proteins, this suggests that one caveolin-binding motif is sufficient for the characteristic subcellular distribution of the 3a protein and its colocalization with caveolin-1.

By using a yeast two-hybrid approach, we showed a direct interaction between caveolin-1 and 3a. The 3a cytoplasmic domain was sufficient for this interaction. This was further confirmed by using FRET, a non-radiative energy-transfer method that is critically dependent upon the distance and dipole orientations of the donor and acceptor fluorophores, and is taken as evidence of an interaction between them (Xia & Liu, 2001). The interaction between caveolin-1 and 3a was directed by the potential caveolin-binding motifs in the latter protein, as its deletion in the Cyto3a background led to a loss of the FRET signal. Furthermore, no direct interaction was seen in either the yeast two-hybrid or FRET assays between the caveolin-1 and Δ3Cyto3a proteins.

There are two broad roles assigned to caveolin-1. One is a structural role wherein the protein is a major component of caveolae; these membrane microdomains are involved in

non-clathrin-mediated virus uptake into cells (Pelkmans *et al.*, 2001; Anderson *et al.*, 1996). Caveolin has been shown to be associated with the assembly of respiratory syncytial virus and to be incorporated into virus particles during assembly (Brown *et al.*, 2002). Whilst preliminary results suggest that caveolin-1 might also associate with SARS-CoV particles, direct evidence for a role of the 3a protein is lacking (data not shown). Through its interaction with caveolin-1, the 3a protein may regulate virus uptake, as well as the trafficking of structural proteins to the plasma membrane or endomembranes, which are the sites for coronavirus assembly and release (Lai & Holmes, 2001).

Caveolins also function as general negative regulators to inhibit the basal activity of many signalling proteins by sequestering these into caveolae (Razani *et al.*, 2000); the sequestration and inhibition cease on activation of signalling (Okamoto *et al.*, 1998; Smart *et al.*, 1999). Loss of caveolin-1 expression activates the Ras–MAPK pathway and transforms NIH 3T3 cells (Galbiati *et al.*, 2001). Caveolin-1 also regulates nitric oxide production in cells by binding nitric oxide synthases (NOS) (Garcia-Cardena *et al.*, 1997; Felley-Bosco *et al.*, 2002). Nitric oxide is genotoxic and a key regulator of cellular damage, and has been shown to inhbit SARS-CoV replication (Akerstrom *et al.*, 2005). We therefore tested whether expression of the 3a protein modulated the ERK and iNOS signalling pathways. No significant effects were observed (results not shown).

In summary, we have used various methods to show that the SARS-CoV 3a protein interacts with caveolin-1. The broad regulatory and structural roles of caveolin-1 in signal transduction (Razani *et al.*, 2000) also demand a more comprehensive analysis of the role of 3a in SARS-CoV pathogenesis.

ACKNOWLEDGEMENTS

We thank Vincent Chow (National University of Singapore) for the *orf3a* gene, Satyajit Mayor (National Centre for Biological Science, Bangalore, India) for the *Cav-1–EGFP* construct and Asutosh Chaudhary and Satyajit Rath for help with the iNOS experiment. We are also grateful to Sia Sin Fun and Mavis H. S. Wu for their assistance in the SARS-CoV experiments. This work was supported by grants from DBT, Government of India (to S. J.) and a grant from the Research Fund for Control of Infectious Diseases, Government of Hong Kong (to J. S. M. P.). ICGEB also receives infrastructural support from the DBT. The awards of Junior Research Fellowships to K. P. and A. H. from CSIR and UGC (India), respectively, are gratefully acknowledged.

REFERENCES

Akerstrom, S., Mousavi-Jazi, M., Klingstrom, J., Leijon, M., Lundkvist, A. & Mirazimi, A. (2005). Nitric oxide inhibits the replication cycle of severe acute respiratory syndrome coronavirus. *J Virol* **79**, 1966–1969.

Anderson, R. G. W. (1998). The caveolae membrane system. *Annu Rev Biochem* **67**, 199–225.

Anderson, H. A., Chen, Y. & Norkin, L. C. (1996). Bound simian virus 40 translocates to caveolin-enriched membrane domains, and its entry is inhibited by drugs that selectively disrupt caveolae. *Mol Biol Cell* **7**, 1825–1834.

Brown, G., Aitken, J., Rixon, H. W. McL. & Sugrue, R. J. (2002). Caveolin-1 is incorporated into mature respiratory syncytial virus particles during virus assembly on the surface of virus-infected cells. *J Gen Virol* **83**, 611–621.

Cai, Q. C., Jiang, Q. W., Zhao, G. M., Guo, Q., Cao, G. W. & Chen, T. (2003). Putative caveolin-binding sites in SARS-CoV proteins. *Acta Pharmacol Sin* **24**, 1051–1059.

Cherukuri, A., Tzeng, S. J., Gidwani, A., Sohn, H. W., Tolar, P., Snyder, M. D. & Pierce, S. K. (2004). Isolation of lipid rafts from B lymphocytes. *Methods Mol Biol* **271**, 213–224.

de Haan, C. A., Smeets, M., Vernooij, F., Vennema, H. & Rottier, P. J. (1999). Mapping of the coronavirus membrane protein domains involved in interaction with the spike protein. *J Virol* **73**, 7441–7452.

Engelman, J. A., Chu, C., Lin, A., Jo, H., Ikezu, T., Okamoto, T., Kohtz, D. S. & Lisanti, M. P. (1998). Caveolin-mediated regulation of signaling along the p42/44 MAP kinase cascade in vivo. A role for the caveolin-scaffolding domain. *FEBS Lett* **428**, 205–211.

Engelman, J. A., Zhang, X. L., Razani, B., Pestell, R. G. & Lisanti, M. P. (1999). p42/44 MAP kinase-dependent and -independent signaling pathways regulate caveolin-1 gene expression. Activation of Ras-MAP kinase and protein kinase A signaling cascades transcriptionally down-regulates caveolin-1 promoter activity. *J Biol Chem* **274**, 32333–32341.

Felley-Bosco, E., Bender, F. & Quest, A. F. (2002). Caveolin-1-mediated post transcriptional regulation of inducible nitric oxide synthase in human colon carcinoma cells. *Biol Res* **35**, 169–176.

Fetzer, C., Tews, B. A. & Meyers, G. (2005). The carboxy-terminal sequence of the pestivirus glycoprotein E^{rns} represents an unusual type of membrane anchor. *J Virol* **79**, 11901–11913.

Galbiati, F., Volonte, D., Liu, J., Capozza, F., Frank, P. G., Zhu, L., Pestell, R. G. & Lisanti, M. P. (2001). Caveolin-1 expression negatively regulates cell cycle progression by inducing G(0)/G(1) arrest via a p53/p21(WAF1/Cip1)-dependent mechanism. *Mol Biol Cell* **12**, 2229–2244.

Garcia-Cardena, G., Martasek, P., Masters, B. S., Skidd, P. M., Couet, J., Li, S., Lisanti, M. P. & Sessa, W. C. (1997). Dissecting the interaction between nitric oxide synthase (NOS) and caveolin. Functional significance of the NOS caveolin binding domain *in vivo*. *J Biol Chem* **272**, 25437–25440.

Holmes, K. V. (2003). SARS coronavirus: a new challenge for prevention and therapy. *J Clin Invest* **111**, 1605–1609.

Huang, C., Narayanan, K., Ito, N., Peters, C. J. & Makino, S. (2006). Severe acute respiratory syndrome coronavirus 3a protein is released in membranous structures from 3a protein-expressing cells and infected cells. *J Virol* **80**, 210–217.

Hulit, J., Bash, T., Fu, M., Galbiati, F., Albanese, C., Sage, D. R., Schlegel, A., Zhurinsky, J., Shtutman, M. & other authors (2000). The cyclin D1 gene is transcriptionally repressed by caveolin-1. *J Biol Chem* **275**, 21203–21209.

Ito, N., Mossel, E. C., Narayanan, K., Popov, V. L., Huang, C., Inoue, T., Peters, C. J. & Makino, S. (2005). Severe acute respiratory syndrome coronavirus 3a protein is a viral structural protein. *J Virol* **79**, 3182–3186.

Jameel, S., Zafrullah, M., Ozdener, M. H. & Panda, S. K. (1996). Expression in animal cells and characterization of the hepatitis E virus structural proteins. *J Virol* **70**, 207–216.

Kar-Roy, A., Korkaya, H., Oberoi, R., Lal, S. K. & Jameel, S. (2004). The hepatitis E virus open reading frame 3 protein activates ERK through binding and inhibition of the MAPK phosphatase. *J Biol Chem* **279**, 28345–28357.

Ksiazek, T. G., Erdman, D., Goldsmith, C. S., Zaki, S. R., Peret, T., Emery, S., Tong, S., Urbani, C., Comer, J. A. & other authors (2003). A novel coronavirus associated with severe acute respiratory syndrome. *N Engl J Med* **348**, 1953–1966.

Lai, M. M. C. & Holmes, K. V. (2001). *Coronaviridae*: the viruses and their replication. In *Fields Virology*, 4th edn, pp. 1163–1185. Edited by B. Fields, D. M. Knipe & P. M. Howley. Philadelphia, PA: Lippincott Williams & Wilkins.

Law, P. T., Wong, C. H., Au, T. C., Chuck, C. P., Kong, S. K., Chan, P. K., To, K. F., Lo, A. W., Chan, J. Y. & other authors (2005). The 3a protein of severe acute respiratory syndrome-associated coronavirus induces apoptosis in Vero E6 cells. *J Gen Virol* **86**, 1921–1930.

Li, S., Couet, J. & Lisanti, M. P. (1996). Src tyrosine kinases, G-alpha subunits, and H-Ras share a common membrane-anchored scaffolding protein, caveolin. Caveolin binding negatively regulates the autoactivation of Src tyrosine kinases. *J Biol Chem* **271**, 29182–29190.

Lisanti, M. P., Scherer, P., Tang, Z.-L. & Sargiacomo, M. (1994). Caveolae, caveolin and caveolin-rich membrane domains: a signaling hypothesis. *Trends Cell Biol* **4**, 231–235.

Lu, W., Zheng, B. J., Xu, K., Schwartz, W., Du, L., Wong, C. K., Chen, J., Duan, S., Deubel, V. & Sun, B. (2006). Severe acute respiratory syndrome-associated coronavirus 3a protein forms an ion channel and modulates virus release. *Proc Natl Acad Sci U S A* **103**, 12540–12545.

Marra, M. A., Jones, S. J., Astell, C. R., Holt, R. A., Brooks-Wilson, A., Butterfield, Y. S., Khattra, J., Asano, J. K., Barber, S. A. & other authors (2003). The genome sequence of the SARS-associated coronavirus. *Science* **300**, 1399–1404.

Murata, M., Peranen, J., Schreiner, R., Wieland, F., Kurzchalia, T. V. & Simons, K. (1995). VIP21/caveolin is a cholesterol-binding protein. *Proc Natl Acad Sci U S A* **92**, 10339–10343.

Navas-Martin, S. & Weiss, S. R. (2003). SARS: lessons learned from other coronaviruses. *Viral Immunol* **16**, 461–474.

Okamoto, T., Schlegel, A., Scherer, P. E. & Lisanti, M. P. (1998). Caveolins, a family of scaffolding proteins for organizing "pre-assembled signaling complexes" at the plasma membrane. *J Biol Chem* **273**, 5419–5422.

Oostra, M., de Haan, C. A. M., de Groot, R. J. & Rottier, P. J. M. (2006). Glycosylation of the severe acute respiratory syndrome coronavirus triple-spanning membrane proteins 3a and M. *J Virol* **80**, 2326–2336.

Ortego, J., Sola, I., Almazan, F., Ceriani, J. E., Riquelme, C., Balasch, M., Plana, J. & Enjuanes, L. (2003). Transmissible gastroenteritis coronavirus gene 7 is not essential but influences in vivo virus replication and virulence. *Virology* **308**, 13–22.

Paul, P. S., Vaughn, E. M. & Halbur, P. G. (1997). Pathogenicity and sequence analysis studies suggest potential role of gene 3 in virulence of swine enteric and respiratory coronaviruses. *Adv Exp Med Biol* **412**, 317–321.

Pelkmans, L., Kartenbeck, J. & Helenius, A. (2001). Caveolar endocytosis of simian virus 40 reveals a new two-step vesicular-transport pathway to the ER. *Nat Cell Biol* **3**, 473–483.

Pendleton, A. R. & Machamer, C. E. (2005). Infectious bronchitis virus 3a protein localizes to a novel domain of the smooth endoplasmic reticulum. *J Virol* **79**, 6142–6151.

Razani, B., Schlegel, A. & Lisanti, M. P. (2000). Caveolin proteins in signaling, oncogenic transformation and muscular dystrophy. *J Cell Sci* **113**, 2103–2109.

Rota, P. A., Obertse, M. S., Monroe, S. S., Nix, W. A., Campagnoli, R., Icenogle, J. P., Peñaranda, S., Bankamp, B., Maher, K. & other authors (2003). Characterization of a novel coronavirus associated with severe acute respiratory syndrome. *Science* **300**, 1394–1399.

Rothberg, K. G., Heuser, J. E., Donzell, W. C., Ying, Y. S., Glenney, J. R. & Anderson, R. G. (1992). Caveolin, a protein component of caveolae membrane coats. *Cell* **68**, 673–682.

Sargiacomo, M., Sudol, M., Tang, Z. & Lisanti, M. P. (1993). Signal transducing molecules and glycosyl-phosphatidylinositol-linked proteins form a caveolin-rich insoluble complex in MDCK cells. *J Cell Biol* **122**, 789–807.

Sargiacomo, M., Scherer, P. E., Tang, Z., Kubler, E., Song, K. S., Sanders, M. C. & Lisanti, M. P. (1995). Oligomeric structure of caveolin: implications for caveolae membrane organization. *Proc Natl Acad Sci U S A* **92**, 9407–9411.

Schlegel, A. & Lisanti, M. P. (2000). A molecular dissection of caveolin-1 membrane attachment and oligomerization. Two separate regions of the caveolin-1 C-terminal domain mediate membrane binding and oligomer/oligomer interactions *in vivo*. *J Biol Chem* **275**, 21605–21617.

Schlegel, A., Schwab, R. B., Scherer, P. E. & Lisanti, M. P. (1999). A role for the caveolin scaffolding domain in mediating the membrane attachment of caveolin-1. The caveolin scaffolding domain is both necessary and sufficient for membrane binding *in vitro*. *J Biol Chem* **274**, 22660–22667.

Shen, S., Lin, P. S., Chao, Y. C., Zhang, A., Yang, X., Lim, S. G., Hong, W. & Tan, Y. J. (2005). The severe acute respiratory syndrome coronavirus 3a is a novel structural protein. *Biochem Biophys Res Commun* **330**, 286–292.

Siegel, R. M., Chan, F. K.-M., Zacharias, D. A., Swofford, R., Holmes, K. L., Tsien, R. Y. & Lenardo, M. J. (2000). Measurement of molecular interactions in living cells by fluorescence resonance energy transfer between variants of the green fluorescent protein. *Sci STKE* **2000** (38), PL1.

Smart, E. J., Graf, G. A., McNiven, M. A., Sessa, W. C., Engelman, J. A., Scherer, P. E., Okamoto, T. & Lisanti, M. P. (1999). Caveolins, liquid-ordered domains, and signal transduction. *Mol Cell Biol* **19**, 7289–7304.

Tan, Y. J., Goh, P. Y., Fielding, B. C., Shen, S., Chou, C. F., Fu, J. L., Leong, H. N., Leo, Y. S., Ooi, E. E. & other authors (2004a). Profiles of antibody responses against severe acute respiratory syndrome coronavirus recombinant proteins and their potential use as diagnostic markers. *Clin Diagn Lab Immunol* **11**, 362–371.

Tan, Y. J., Teng, E., Shen, S., Tan, T. H., Goh, P. Y., Fielding, B. C., Ooi, E. E., Tan, H. C., Lim, S. G. & Hong, W. (2004b). A novel severe acute respiratory syndrome coronavirus protein, U274, is transported to the cell surface and undergoes endocytosis. *J Virol* **78**, 6723–6734.

Tan, Y. J., Tham, P. Y., Chan, D. Z., Chou, C. F., Shen, S., Fielding, B. C., Tan, T. H., Lim, S. G. & Hong, W. (2005). The severe acute respiratory syndrome coronavirus 3a protein up-regulates expression of fibrinogen in lung epithelial cells. *J Virol* **79**, 10083–10087.

Tyagi, S., Surjit, M., Kar-Roy, A., Jameel, S. & Lal, S. K. (2004). The ORF3 protein of hepatitis E virus interacts with liver-specific α_1-microglobulin and its precursor, α_1-microglobulin/bikunin precursor (AMBP) and expedites their export from the hepatocyte. *J Biol Chem* **279**, 29308–29319.

Vaughn, E. M., Halbur, P. G. & Paul, P. S. (1995). Sequence comparison of porcine respiratory coronavirus isolates reveals heterogeneity in the S, 3, and 3–1 genes. *J Virol* **69**, 3176–3184.

Wesley, R. D., Woods, R. D. & Cheung, A. K. (1991). Genetic analysis of porcine respiratory coronavirus, an attenuated variant of transmissible gastroenteritis virus. *J Virol* **65**, 3369–3373.

Xia, Z. & Liu, Y. (2001). Reliable and global measurement of fluorescence resonance energy transfer using fluorescence microscopes. *Biophys J* **81**, 2395–2402.

Yount, B., Roberts, R. S., Sims, A. C., Deming, D., Frieman, M. B., Sparks, J., Denison, M. R., Davis, N. & Baric, R. S. (2005). Severe acute respiratory syndrome coronavirus group-specific open reading frames encode nonessential functions for replication in cell cultures and mice. *J Virol* **79**, 14909–14922.

Yu, C. J., Chen, Y. C., Hsiao, C. H., Kuo, T. C., Chang, S. C., Lu, C. Y., Wei, W. C., Lee, C. H., Huang, L. M. & other authors (2004). Identification of a novel protein 3a from severe acute respiratory syndrome coronavirus. *FEBS Lett* **565**, 111–116.

Yuan, X., Li, J., Shan, Y., Yang, Z., Zhao, Z., Chen, B., Yao, Z., Dong, B., Wang, S. & other authors (2005). Subcellular localization and membrane association of SARS-CoV 3a protein. *Virus Res* **109**, 191–202.

Zafrullah, M., Ozdener, M. H., Kumar, R., Panda, S. K. & Jameel, S. (1999). Mutational analysis of glycosylation, membrane translocation, and cell surface expression of the hepatitis E virus ORF2 protein. *J Virol* **73**, 4074–4082.

Zeng, R., Yang, R.-F., Shi, M.-D., Jiang, M. R., Xie, Y. H., Ruan, H. Q., Jiang, X. S., Shi, L., Zhou, H. & other authors (2004). Characterization of the 3a protein of SARS-associated coronavirus in infected vero E6 cells and SARS patients. *J Mol Biol* **341**, 271–279.